arXiv:physics/9806035v1 [physics.class-ph] 22 Jun 1998

Construction of Simulation Wavefunctions for Aqueous Species: D_3O^+

M. A. Gomez and L. R. Pratt
Theoretical Division Los Alamos National Laboratory, Los Alamos, New Mexico 87545 USA

LA-UR-98-2692
(May 1, 2019)

Abstract

This paper investigates Monte Carlo techniques for construction of compact wavefunctions for the internal atomic motion of the D_3O^+ ion. The polarization force field models of Stillinger, *et al.* and of Ojamae, *et al.* were used. Initial pair product wavefunctions were obtained from the asymptotic high temperature many-body density matrix after contraction to atom pairs using Metropolis Monte Carlo. Subsequent characterization shows these pair product wavefunctions to be well optimized for atom pair correlations despite that fact that the predicted zero point energies are too high. The pair product wavefunctions are suitable to use within variational Monte Carlo, including excited states, and density matrix Monte Carlo calculations. Together with the pair product wavefunctions, the traditional variational theorem permits identification of wavefunction features with significant potential for further optimization. The most important explicit correlation variable found for the D_3O^+ ion was the vector triple product $\mathbf{r}_{OD1}\cdot(\mathbf{r}_{OD2}\times\mathbf{r}_{OD3})$. Variational Monte Carlo with 9 of such explicitly correlated functions yielded a ground state wavefunction with an error of 5-6% in the zero point energy.

INTRODUCTION

Flexible and dissociative models for simulation of liquid water have often been used in classical statistical mechanical studies of aqueous materials. [1–35] They present technical advantages for carrying-out simulations and are of-the-essence where dissociation of water molecules is necessary to the chemistry being studied. Studies of clusters suggest that quantum mechanics plays a non-negligible role in proton transfer. [36] However, directly incorporating quantum mechanics via discretized path integral approaches may require one or more orders of magnitude larger computational effort. [37] This Report investigates constructing simple intramolecular wavefunctions for aqueous species. These wavefunctions might be used in Monte Carlo simulations of aqueous solutions with the same computational techniques used to treat flexible simulation models classically. More specifically, our goal is to determine the complication and accuracy to be expected in constructing wavefunctions that might be transferrable and useful in related studies of aqueous solution chemistry.

We take the deuterated hydronium ion, D_3O^+, as a specific example species. We choose this ion because of the substantial current interest in proton exchange processes in water and in the spectroscopy of charged clusters of water molecules; [1,23,35,36,38–40] we choose the deuterated case to avoid the interesting complications of spin restrictions on the wavefunctions. In addition we will study here only states of zero angular momentum, J=0. Our goal will be to obtain a simple intramolecular wavefunction for this species in a reasonably organized fashion.

A traditional exhaustive expansion of the wavefunction into a basis will produce satisfactory vibrational energies with effort but is unlikely to produce a simple result for the wavefunction. Less traditionally, diffusion Monte Carlo [41] will produce satisfactory vibrational energies for low energy states with effort but not a simple wavefunction for other uses.

In contrast, the historical work of McMillan [42], a variational Monte Carlo calculation for the ground state of liquid He^4, does directly center on the construction of a simple wavefunction. The Monte Carlo character of this technique is limited to the primitive but essential task of evaluating integrals with a many-body wavefunction. This approach permits simple but sophisticated descriptions of correlation and can include a limited number of excited states. The possibility of simultaneous treatment of excited states provides an additional avenue for description of correlation. In fact, the density matrix Monte Carlo approach [41,43–45] of recent years can be regarded as a generalization of the McMillan calculation; the β=0 circumstance is precisely the result that we view as the McMillan calculation with excited states.

The full power of the density matrix Monte Carlo approach can be used with rough initial estimates of the wavefunctions sought. The Monte Carlo calculation systematically improves the computed energy levels. However, since our goal is to derive a wavefunction useful in other contexts, we emphasize finding and utilizing the best simple function we can before the density matrix Monte Carlo procedure takes over.

We will initially use pair-product wavefuctions for atomic motion. The components of the pair-product are obtained by diagonalizing an approximate density matrix. We emphasize that initial models of a set of vibrational wavefunctions need not be orthonormal. The possibility of using functions localized in different conformational basins provides a well-

defined analysis of zero-point effects on conformational equilibria.

It is found (below) that these initial pair-product wavefunctions capture two body correlations fairly well. Using them as a basis in McMillan and density matrix Monte Carlo calculations incorporates further correlation effects. To obtain more compact wavefunctions, the variational principle is used to identify the important many-body correlations. These effects are included into the ground state wavefunction and yield a significantly improved simple wavefunction for the ground state. A few of these correlated wavefunctions can be used as the basis in a McMillan calculation yielding reasonably accurate wavefunctions.

MODEL WAVEFUNCTIONS FOR ATOMIC MOTION

We develop the vibrational wavefunctions analogously to development of wavefunctions for liquid He. We initially seek a pair product form

$$\Phi_0 = \prod_{OD\ pairs} \phi_{OD}(r_{OD}) \prod_{DD\ pairs} \phi_{DD}(r_{DD}) \ . \tag{1}$$

In this case, we expect the functions ϕ_{OD} to be local mode orbitals and the functions ϕ_{DD} to serve as correlation functions.

The casual interpretation of these functions as orbitals will serve to distinguish vibrational excitations. The method sketched here is based upon the observation that the eigenfunctions of the asymptotic $\beta \to 0$ density matrix are suitable initial estimates of the pair functions sought. This method has the additional advantage that harmonic analysis of a potentially rough energy landscape is not required.

We start with a function of this simple form for several reasons. First, a similar distribution is implied when flexible and dissociative pair simulation models of water are treated classically. Second, elements of such a form might be approximately transferrable to OD and DD joint distributions in other settings - this would be the common assumption for simulation calculations. Third, such a form would be similar, though not the same as a ground state vibrational wavefunction for a harmonic system. The distinctions are that normal modes coordinates are not used, and that functions employed can attempt to treat anharmonic systems by deviating from Gaussian form where the potential is anharmonic. The remainder of this paper characterizes such wavefunctions and investigates some improvements.

Natural orbitals for general oscillators in one dimension

If the density matrix $\langle x'; \beta | x \rangle \equiv < x' | e^{-\beta H} | x >$ were known, its natural orbitals would be obtained from

$$\int \langle x'; \beta | x \rangle \phi_n(x') dx' = e^{-\beta E_n} \phi_n(x) \tag{2}$$

In fact the asymptotic $\beta \to 0$ limit of the density matrix is simple: [46]

$$\langle x'; \beta | x \rangle = (m/2\pi\beta\hbar^2)^{1/2} \exp\{-m(x-x')^2/2\beta\hbar^2 - \beta(V(x)+V(x'))/2\} \ . \tag{3}$$

Sethia *et al.* showed that though the density matrix used is approximate, satisfactory orbital functions are obtained. [47] This form for the thermal density matrix is more than merely

an approximation. For small β, it is asymptotically correct. Therefore, it is satisfactory if the application permits a small β. The subsequent developments exploit this point.

Contraction to Pairs for the many-body Thermal Density Matrix

For higher dimensional problems, we can exploit the approximate density matrix to produce the necessary reasonable pair functions after tracing-out all other degrees of freedom. This tracing-out will be generally possible on the basis of classical Monte Carlo techniques.

Consider a system composed of N particles located at $(\mathbf{r}_1, \mathbf{r}_2 \ldots \mathbf{r}_N)$. The N-body high-temperature thermal density matrix is

$$\langle \mathbf{r}_1, \mathbf{r}_2 \ldots \mathbf{r}_N; \beta | \mathbf{r'}_1, \mathbf{r'}_2 \ldots \mathbf{r'}_N \rangle = \prod_{k=1}^{N} (m_k/2\pi\beta\hbar^2)^{3/2} \exp\{-m_k(\mathbf{r}_k - \mathbf{r'}_k)^2/2\beta\hbar^2\} \times \exp\{-\beta(V(\mathbf{r}_1, \mathbf{r}_2 \ldots \mathbf{r}_N) + V(\mathbf{r'}_1, \mathbf{r'}_2 \ldots \mathbf{r'}_N))/2\} \ . \quad (4)$$

We now focus on the {ij} pair of particles. For all other particles, we restrict the density matrix to the diagonal. For example, taking {ij}={12} we obtain

$$\langle \mathbf{r}_1, \mathbf{r}_2 \ldots \mathbf{r}_N; \beta | \mathbf{r'}_1, \mathbf{r'}_2 \ldots \mathbf{r}_N \rangle \propto \prod_{k=1,2} (m_k/2\pi\beta\hbar^2)^{3/2} \exp\{-m_k(\mathbf{r}_k - \mathbf{r'}_k)^2/2\beta\hbar^2\} \times \exp\{-\beta(V(\mathbf{r}_1, \mathbf{r}_2 \ldots \mathbf{r}_N) + V(\mathbf{r'}_1, \mathbf{r'}_2 \ldots \mathbf{r}_N))/2\}. \quad (5)$$

where we have dropped some irrelevant multiplicative constants. Now for the {12} pair we transform to the {12} center of mass and relative coordinates: $\mathbf{R} = (m_1\mathbf{r}_1 + m_2\mathbf{r}_2)/(m_1+m_2)$ and $\mathbf{r} = \mathbf{r}_1 - \mathbf{r}_2$.

$$\langle \mathbf{R} + m_2\mathbf{r}/M, \mathbf{R} - m_1\mathbf{r}/M \ldots \mathbf{r}_N; \beta | \mathbf{R'} + m_2\mathbf{r'}/M, \mathbf{R'} - m_1\mathbf{r'}/M \ldots \mathbf{r}_N \rangle \propto \exp\{-\beta(V(\mathbf{R} + m_2\mathbf{r}/M, \mathbf{R} - m_1\mathbf{r}/M \ldots \mathbf{r}_N) + V(\mathbf{R'} + m_2\mathbf{r'}/M, \mathbf{R'} - m_1\mathbf{r'}/M \ldots \mathbf{r}_N))/2\} \times (M/2\pi\beta\hbar^2)^{3/2} \exp\{-M(\mathbf{R} - \mathbf{R'})^2/2\beta\hbar^2\} (\mu/2\pi\beta\hbar^2)^{3/2} \exp\{-\mu(\mathbf{r} - \mathbf{r'})^2/2\beta\hbar^2\}. \quad (6)$$

where we have used the notation $M = m_1 + m_2$ and $\mu = m_1 m_2/M$.

Note that R is not the molecular center of mass and that the potential generally does depend on R. However, in the interest of simplicity and in view of the form sought Eq. (1), we will trace-out the R dependence also. Our final step will be to use classical Monte Carlo techniques for the integrations required to bring Eq. (6) into the form of Eq.(2) for the relative coordinate r. Thus we sample configurations with the probability density $\exp\{-\beta V(\mathbf{r}_1, \mathbf{r}_2 \ldots \mathbf{r}_N)\}$ and we estimate the kernel

$$K(\mathbf{r}, \mathbf{r'}) \propto \left\langle e^{-\mu(\mathbf{r}_1 - \mathbf{r}_2 - \mathbf{r'})^2/2\beta\hbar^2} \delta(\mathbf{r} - \mathbf{r}_1 + \mathbf{r}_2) e^{-\beta\delta V(\mathbf{R} + m_2\mathbf{r'}/M, \mathbf{R} - m_1\mathbf{r'}/M \ldots \mathbf{r}_N)/2} \right\rangle_{e^{-\beta V}} , \quad (7)$$

where

$$\delta V(\mathbf{R} + m_2\mathbf{r'}/M, \mathbf{R} - m_1\mathbf{r'}/M \ldots \mathbf{r}_N) \equiv V([m_1\mathbf{r}_1 + m_2\mathbf{r}_2 + m_2\mathbf{r'}]/M, [m_1\mathbf{r}_1 + m_2\mathbf{r}_2 - m_1\mathbf{r'}]/M \ldots \mathbf{r}_N) - V(\mathbf{r}_1, \mathbf{r}_2 \ldots \mathbf{r}_N) \quad (8)$$

$K(\mathbf{r}, \mathbf{r'})$ is symmetric, though the formula Eq. (7) is asymmetric. For the case considered here, it does not depend on the angles that $\mathbf{r}$ or $\mathbf{r'}$ make with the laboratory fixed coordinate

system. Thus, this kernel depends only on r, r′, and the angle between them. Since we here focus on radial functions, we only need the kernel after having averaged over that polar angle.

Note that for determination of the orbitals only, the normalization of the kernel $K(\mathbf{r}, \mathbf{r}')$ is not significant. To within an unimportant normalization constant we can evaluate the required kernel through the following procedure:

1. Draw configurations $(\mathbf{r}_1, \mathbf{r}_2 \ldots \mathbf{r}_N)$ from the probability distribution proportional to $\exp\{-\beta V(\mathbf{r}_1, \mathbf{r}_2 \ldots \mathbf{r}_N)\}$ utilizing the Metropolis Monte Carlo algorithm [48,49].

2. For each configuration, choose an r' from a grid and its corresponding spherical angles θ' and ϕ' using quasi-random number series. Weight each configuration $(\mathbf{r}_1, \mathbf{r}_2 \ldots \mathbf{r}_N)$ and the corresponding $\mathbf{r}'$ by

$$e^{-\mu(\mathbf{r}_1-\mathbf{r}_2-\mathbf{r}')^2/2\beta\hbar^2} e^{-\beta\delta V([m_1\mathbf{r}_1+m_2\mathbf{r}_2+m_2\mathbf{r}']/M,[m_1\mathbf{r}_1+m_2\mathbf{r}_2-m_1\mathbf{r}']/M\ldots\mathbf{r}_N))/2} \tag{9}$$

3. Perform a final integration over angles

$$\overline{K}(r, r') \propto \int_0^\pi d\theta \int_0^\pi d\theta' \int_0^{2\pi} d\phi' \int_0^{2\pi} d\phi \ \sin\theta \ K(\mathbf{r}, \mathbf{r}') \ \sin\theta' \tag{10}$$

   θ, ϕ, θ', and ϕ' are the spherical, angles corresponding to $\mathbf{r}$ and $\mathbf{r}'$. For this case of $J = 0$, it would have been sufficient to integrate over the angle between $\mathbf{r}$ and $\mathbf{r}'$.

With this kernel in hand, we solve the one dimensional equation

$$\int_0^\infty \overline{K}(R, R') R'^2 \phi(R') dr' = \lambda\phi(R) \ . \tag{11}$$

λ is not $e^{-\beta E}$ but is proportional to it.

This approach is not limited to the circumstances that one member of that pair is a massive molecular center. This can be applied also for DD pairs in the D_3O^+ molecule. However, for the D_3O^+ molecule in particular, it is natural to regard the OD functions as local mode orbitals and the DD functions as providing a subsequent account of correlations.

D_3O^+ PAIR FUNCTIONS

The functions ϕ_{OD} and ϕ_{DD} are found for the second version of the Ojamae-Shavitt-Singer (OSS) potential [35] using β^{-1}=0.01 Hartree and a sample size of 500,000 $(\mathbf{r}_1, \mathbf{r}_2 \ldots \mathbf{r}_N)$ configurations. This energy parameter is 6.3 kcal/mole (more than 3000 K), a value above the D_3O^+ inversion barrier of 4.4 kcal/mole. Smaller values for β are problematical because of the fragmentation of the D_3O^+ molecule at high temperatures.

Figure 1 shows ϕ_{DD} obtained. The additional approximation of fixing one of the deuterons in the reference bond has the significant effect of narrowing the pair function. As expected, the effect is not as dramatic for fixing an oxygen atom. The co-linear assumption of fixing the orientation of the reference bond is not significant.

These functions were also obtained for the Stillinger, Stillinger, Hogdgon (SSH) potential. [50] A comparison of features of SSH and OSS is presented in Table I. The higher (more realistic) binding energy for the additional proton in the SSH case and the higher inversion barrier of this potential permits a smaller β. In that case, the pair functions are found for two values of $1/\beta$, namely 0.01 Hartree and 0.01677... Hartree. The difference in the "frequencies" associated with the ground and first excited state OD "local mode" functions changed from 3150 cm^{-1} to 1987 cm^{-1}. The corresponding differences in DD frequencies changed from 1243 cm^{-1} to 837 cm^{-1}. In spite of these large frequency changes, the pair functions, seen in Figure 2, are qualitatively similar.

ACCURACY OF THE PAIR PRODUCT WAVEFUNCTIONS

The numerical arrays describing the OD and DD functions were fit to cubic splines with first derivatives set to zero at the end points [51] and the pair product wavefunctions of Eq. (1) were obtained. Several steps were taken the assess the quality of these wavefunctions. For the OSS and SSH potentials, the variational Monte Carlo [42] zero point energies of the pair product wavefunctions are 0.0321(2) and 0.0367(6) Hartrees, respectively. Simple diffusion Monte Carlo [41] zero-point energies for the potentials are 0.02516(3) and 0.03042(3) Hartrees. (All errors are two standard deviations unless otherwise noted.) The energy for the pair product function is between 20% and 30% too large. This function was further optimized by introducing parameters to move (m) and scale (s) the pair functions; $\phi(r_{new}) = \phi((r_{old} + m)/s)$. No significant lowering of the energy was found.

The quality of optimization of these pair functions can be analyzed directly. The usual variation principle can be expressed as

$$\langle (\delta \ln \Psi)\, E_L(1..N)\rangle_{|\Psi|^2} - \langle (\delta \ln \Psi)\rangle_{|\Psi|^2} \langle E_L(1..N)\rangle_{|\Psi|^2} = 0 \ , \tag{12}$$

where $E_L = \Psi^{-1} H \Psi$ is the usual local energy function and the subscripted brackets $\langle \ldots \rangle_{|\Psi|^2}$ indicate an average with probability density $|\Psi|^2$. For a pair product wavefunction this form implies

$$1 - \frac{\left\langle \hat{\rho}^{(2)}_{\gamma\nu}(r) E_L(1..N)\right\rangle_{|\Psi|^2}}{\left\langle \hat{\rho}^{(2)}_{\gamma\nu}(r)\right\rangle_{|\Psi|^2} \langle E_L(1..N)\rangle_{|\Psi|^2}} = 0 \ , \tag{13}$$

where $\hat{\rho}^{(2)}_{\gamma\nu}(r)$ is the $\gamma\nu$ pair joint density operator.

This stationary requirement is satisfied for the exact ground state wavefunction since the local energy is spatially constant. Any deviation of the left side of Eqn. 13 from zero will be defined as the optimization deficit.

Figure 3 shows the optimization deficit for the OSS DD pair functions and the DD VMC radial distribution function. The OD functions show similar low optimization deficits; these pair functions lead to accurately uncorrelated pair densities and local energies and are thus well optimized. Note that the largest deficits are at the tails of the distribution. Thus further optimization would require significant effort because of the difficulty of getting statistically significant data for those infrequent events.

CORRELATION BEYOND PAIRS: VARIATIONAL AND DENSITY MATRIX MONTE CARLO

We can use model excited state functions to improve the ground state and get a few low lying states at the same time. A concise expression of these approaches is obtained by focusing on the density matrix. Suppose we have a number of approximate wavefunctions $|\Phi_i\rangle, i = 0, \ldots, N$. By Monte Carlo procedures detailed elsewhere [43,44], we estimate the matrix elements

$$\overline{\rho}_{ij}(\beta) \equiv < \Phi_i | \exp\{-\beta H\} | \Phi_j >, \tag{14}$$

and

$$\overline{H}_{ij}(\beta) \equiv < \Phi_i | H \exp\{-\beta H\} | \Phi_j >, \tag{15}$$

for β not too large. As β gets large, information is lost for highly excited states, so this approach depends on location of an intermediate range of β. $\overline{H}$ and $\overline{\rho}$ are then diagonalized simultaneously. The $|\Phi_i\rangle$ need not be orthonormal initially since Monte Carlo methods will be used to perform the required integrations. The $\beta \to 0$ limit may be viewed as a direct extension of the McMillan [42] approach. The trace of $\overline{\rho}_{ij}$ provides a natural importance function for the Monte Carlo calculation.

To apply these methods to our problem, an ordered set of excited state functions is obtained as follows. The ratio of eigenvalues of the nth function and the ground state, δE_n^{pair}, are used to assign relative energies to the pair product functions. If a pair product consists of one ground state and two first excited states of OD interaction, and two ground states, and a first excited state of the DD interaction, the relative energy assigned to it would be $2 * \delta E_1^{OD} + \delta E_1^{DD}$. These functions are symmetrized with respect to exchange of deuterons.

These functions were used in density matrix Monte Carlo calculations. In its $\beta = 0$ limit, density matrix Monte Carlo mixes the lowest energy functions much like configuration interaction in electronic structure calculations. Tables II and III show the energies obtained in these variational calculations for OSS and SSH potentials, respectively. The guiding function used was $\Psi_{\text{trial}}(q) = \left(\sum_{i=0}^{M} \phi_i(x)^2\right)^{\rho}$ with M=5 and $\rho = \frac{1}{4}$. ρ of $\frac{1}{4}$ is used instead of $\frac{1}{2}$ so that higher states than M are efficiently sampled. Alternatively, M could be made larger. However, the cost of making M larger is higher than the cost of making $\rho = \frac{1}{4}$. Independent estimates for the zero-point energy of 0.02516(3) Hartree (5522(7) /cm) and 0.03042(3) Hartree (6676(7) /cm) are found using diffusion Monte Carlo for the OSS and SSH potentials, respectively. Inclusion of a small number of excited states substantially improves the predicted zero-point energy; the 20-30% error with the pair product wavefunction is reduced to about a 10% error with inclusion of nine states. However, the improvement of this prediction with increasing numbers of excited states is slow. As shown in Tables II and III, inclusion of 94 and 99 states still results in a 4-6% error.

The variational energies are significantly improved by density matrix Monte Carlo as β increases from zero with 9 excited state functions. Including more functions accelerates the convergence. (see Figure 4) Tables IV and V show the energy estimates for lowest 5 symmetric states for OSS and SSH respectively. The average energies and their standard

deviations as a function of β were used in a Marquardt's fit to the function $A + Be^{-\beta/C}$. Error bars were obtained by dividing the configurations used to calculate the matrices into smaller sets, diagonalizing these sets, obtaining the standard deviation for their eigenvalues, and dividing it by the square root of the number of sets. Assuming that the distribution of errors is Gaussian, the ellipsoid representing 90% error can be plotted. [51] The errors reported in Tables IV and V are χ^2 90% confidence intervals. Some data was not well approximated by a decaying exponential. In this case, the point in the plateau with the smallest standard deviation is given. For this data which is designated by a *, 2 standard deviations are given in parenthesis.

Because it is relevant to assessment of potential energy surface models, we note in passing that for the OSS potential the excited vibrational state with a node $\mathbf{r}_{OD1}\cdot(\mathbf{r}_{OD2}\times\mathbf{r}_{OD3}=0$ has an energy of 0.02522(4) Hartree as determined by a fixed node diffusion Monte Carlo calculation. This is about about 15(24) /cm higher than the zero point energy. A model fit to experiment by Sears *et al.* yielded a gap of 15/cm. However, the OSS potential overestimates the inversion barrier and, therefore, we expect it to underestimate this splitting. Beyond this comparison, our results for both the OSS and SSH potential differ signicantly from the results of Sears *et al.* For example, first totally symmetric excited states are 794(10)/cm and 731(11)/cm above the ground state for OSS and SSH respectively. The first totally symmetric excited state in Sears' fit was 453/cm above the ground state. [52]

EXPRESSING CORRELATIONS BEYOND PAIRS MORE COMPACTLY

The variational principle Eq. 12 and the optimization deficit can be used to search for structural variables that are correlated with the local energy. Such variables are principal candidates for construction of explicitly correlated wavefunctions.

Consideration of several natural possibilities for such structural variables identified the coordinate u=$\mathbf{r}_{OD1}\cdot(\mathbf{r}_{OD2}\times\mathbf{r}_{OD3})$ as more correlated with the local energy of the pair product wavefunction than any other combination considered. Therefore, we added a product of the form $e^{f(u)}$ to our pair product wavefunction. The distribution of u and the f(u) optimization deficit (see Fig. 5) with this pair product wavefunction suggested that f(u) take the form

$$\Psi_{\text{n-body}} = e^{-a(u-b)^2} + e^{-a(u+b)^2} \quad . \tag{16}$$

The pair product wavefunction with moving and scaling parameters times this new multiplicative many-body factor was optimized using Variational Monte Carlo. Zero point energies of 0.02838(4) Hartree (6229(9) /cm) and 0.03326(2) Hartree (7300(4) /cm) are obtained for the correlated wavefunctions with the OSS and SSH potentials, respectively. This is nearly as good as the VMC result with mixing of 9 states. The optimized parameters are shown in Table VI. The new distribution and optimization deficit for the OSS potential are shown in Fig. 6.

Using pair product wavefunctions with this correlation piece as the basis in a McMillan VMC calculation with 9 functions reduced the ground state energy to 5860(2) /cm and 7041(3) /cm for OSS and SSH potentials, respectively. These energies contain 5-6% error with respect to the DMC ground state energies.

CONCLUSION

A pair product wavefunction for D_3O^+ has been obtained from an approximate density matrix. This pair product wavefunction captures two body interactions fairly well. Variational Monte Carlo includes correlation by mixing in excited states. However, it takes about 99 states to get to an error of 4-6%. Density Matrix Monte Carlo gets accurate energies with 9 wavefunctions. However, it does not provide a simple wavefunction.

A compact ground state function is obtained by using the variational principle to identify the most significant many-body terms and including it directly into the wavefunction. For the D_3O^+ ion the most significant such variable was the vector triple product $\mathbf{r}_{OD1}\cdot(\mathbf{r}_{OD2}\times\mathbf{r}_{OD3})$. Variational Monte Carlo with 9 of these correlated functions yields a ground state wavefunction with an error of 5-6% in the zero point energy.

ACKNOWLEDGMENTS

We thank the group L. Ojamae, I. Shavitt, and S. J. Singer, and the group F. H. Stillinger, D. K. Stillinger, and J. A. Hodgdon for pre-publication release of their potential energy surfaces. We also thank R. A. Harris and R. B. Walker for helpful discussions. This study was supported by the LDRD program at Los Alamos National Laboratory.

REFERENCES

[1] F. H. Stillinger and C. W. David, J. Chem. Phys. **69**, 1475 (1978).
[2] M. D. Morse and S. A. Rice, J. Chem. Phys. **74**, 6514 (1981).
[3] N. I. Christou, J. S. Whitehouse, D. Nicholson, and N. G. Parsonage, Faraday Sym. Chem. Soc. 139 (1981).
[4] T. A. Weber and F. H. Stillinger, J. Phys. Chem. **86**, 1314 (1982).
[5] J. R. Reimers, R. O. Watts, and M. L. Klein, Chem. Phys. **64**, 95 (1982).
[6] P. H. Berens, D. H. J. Mackay, G. M. White, and K. R. Wilson, J. Chem. Phys. **79**, 2375 (1983).
[7] P. Bopp, G. Jancso, and K. Heinzinger, Chem. Phys. Letts. **98**, 129 (1983).
[8] G. Jancso and P. Bopp, Z. Naturforsch. A **38**, 206 (1983).
[9] O. Teleman, B. Jonsson, and S. Engstrom, Molec. Phys. **60**, 193 (1987).
[10] R. A. Thuraisingham and H. L. Friedman, J. Chem. Phys. **78**, 5772 (1983).
[11] P. W. Deutsch and T. D. Stanik, J. Chem. Phys. **85**, 4660 (1986).
[12] M. J. Wojcik, J. Molec. Struct. **189**, 89 (1988).
[13] A. Wallqvist, Chem. Phys. **148**, 439 (1990).
[14] I. Ruff and D. J. Diestler, J. Chem. Phys. **93**, 2032 (1990).
[15] Z. Slanina, Chem. Phys. Letts. **172**, 367 (1990).
[16] A. Wallqvist and O. Teleman, Molec. Phys. **74**, 515 (1991).
[17] S. B. Zhu *et al.*, J. Phys. Chem. **95**, 6211 (1991).
[18] M. A. Suhm and R. O. Watts, Molec. Phys. **73**, 463 (1991).
[19] L. Ojamae, K. Hermansson, and M. Probst, Chem. Phys. Letts. **191**, 500 (1992).
[20] L. Ojamae, J. Tegenfeldt, J. Lindgren, and K. Hermansson, Chem. Phys. Letts. **195**, 97 (1992).
[21] G. Corongiu, Int. J. Quant. Chem. **42**, 1209 (1992).
[22] D. E. Smith and A. D. J. Haymet, J. Chem. Phys. **96**, 8450 (1992).
[23] J. W. Halley, J. R. Rustad, and A. Rahman, J. Chem. Phys. **98**, 4110 (1993).
[24] G. Corongiu and E. Clementi, J. Chem. Phys. **98**, 4984 (1993).
[25] F. Sciortino and G. Corongiu, J. Chem. Phys. **98**, 5694 (1993).
[26] A. D. Trokhymchuk, M. F. Holovko, and K. Heinzinger, J. Chem. Phys. **99**, 2964 (1993).
[27] M. Vossen and F. Forstmann, J. Chem. Phys. **101**, 2379 (1994).
[28] T. I. Mizan, P. E. Savage, and R. M. Ziff, J. Phys. Chem. **98**, 13067 (1994).
[29] D. M. Duh, D. N. Perera, and A. D. J. Haymet, J. Chem. Phys. **102**, 3736 (1995).
[30] A. G. Kalinichev and K. Heinzinger, Geochim. Cosmochim. Acta **59**, 641 (1995).
[31] C. W. David, J. Chem. Phys. **104**, 7255 (1996).
[32] R. Bansil *et al.*, Chem. Phys. Letts. **132**, 165 (1986).
[33] P. L. Silvestrelli, M. Bernasconi, and M. Parrinello, Chem. Phys. Letts. **277**, 478 (1997).
[34] Y. Liu *et al.*, to be published .
[35] L. Ojamae, I. Shavitt, and S. J. Singer, to be published .
[36] M. E. Tuckerman, D. Marx, M. L. Klein, and M. . Parrinello, Science **275**, 817 (1997).
[37] J. M. Hammersley and D. C. Handscomb, (Chapman and Hall, London, 1964).
[38] R. Pomés and B. Roux, Chem. Phys. Lett. **234**, 416 (1995).
[39] M. Tuckerman, K. Laasonen, M. Sprik, and M. Parrinello, J. Phys. Chem. **99**, 5749 (1995).
[40] R. Pomés and B. Roux, J. Phys. Chem **100**, 2519 (1996).

[41] B. L. Hammond, W. A. Lester, Jr., and P. J. Reynolds, *Monte Carlo Methods in Ab Initio Quantum Chemistry* (World Scientific, River Edge, NJ, USA, 1994).
[42] W. L. McMillan, Phys. Rev. A **138**, 442 (1965).
[43] D. M. Ceperley and B. Bernu, J. Chem. Phys. **89**, 6316 (1988).
[44] B. Bernu, D. M. Ceperley, and W. A. Lester, Jr., J. Chem. Phys. **93**, 552 (1990).
[45] W. R. Brown, W. A. Glauser, and W. A. Lester, Jr., J. Chem. Phys. **103**, 9721 (1995).
[46] R. P. Feynman, *Statistical Mechanics, A Set of Lectures* (Benjamin, Reading, Massachusetts, 1972), see chapter 3.
[47] A. Sethia, S. Sanyal, and Y. Singh, J. Chem. Phys. **93**, 7268 (1990).
[48] N. Metropolis *et al.*, J. Chem. Phys. **21**, 1087 (1953).
[49] M. H. Kalos and P. A. Whitlock, *Monte Carlo Methods, Volume I: Basics* (John Wiley and Sons, New York, 1986).
[50] F. H. Stillinger, D. K. Stillinger, and J. A. Hodgdon, preprint .
[51] W. H. Press, S. A. Teukolsky, W. T. Vetterling, and B. P. Flannery, *Numerical Recipies in C: The Art of Scientific Computing, Second Edition* (Cambridge University Press, Cambridge, 1992), pp. 113–116.
[52] T. J. Sears *et al.*, J. Chem. Phys. **83**, 2576 (1985).

FIGURES

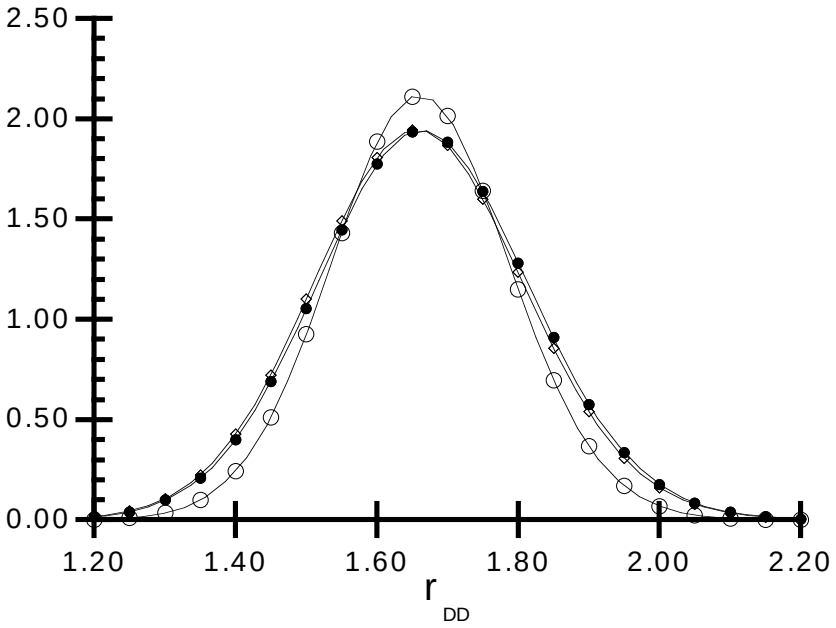

FIG. 1. The $\phi(r_{\mathrm{DD}})$ obtained by fixing one of the deuterons (line with open circles) is significantly narrower than that obtained from unconstrained sampling (line with diamonds). The co-linear assumption of fixing the orientation of the reference bond (line with solid circles) is not significant. The points were fit to cubic splines. Displacements are in Å .

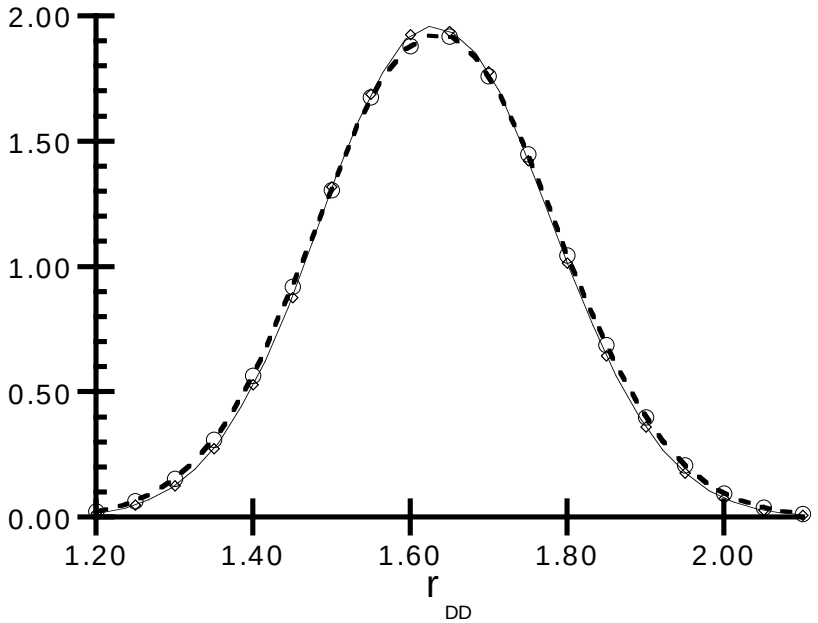

FIG. 2. The $\phi(r_{\rm DD})$ obtained using $1/\beta$=0.01677... Hartree (open circles on dashed line) is slightly wider than that obtained using $1/\beta$=0.01 Hartree (diamonds on solid line). The points were fit to cubic splines. Displacements are in Å .

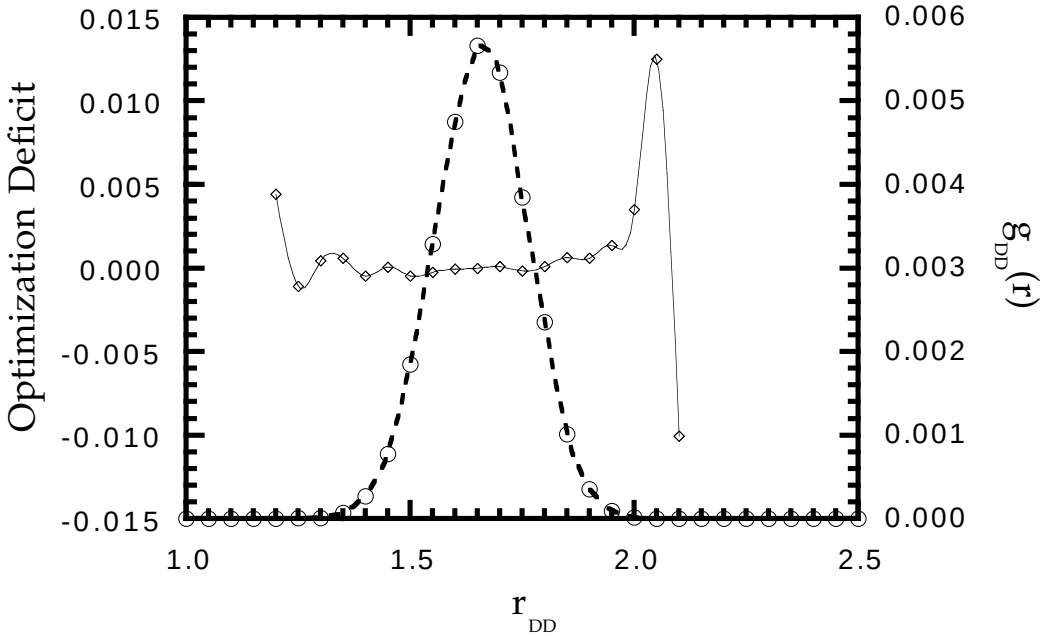

FIG. 3. DD optimization deficit (diamonds on solid line) and VMC radial distribution function (open circles on dashed line) for OSS model.

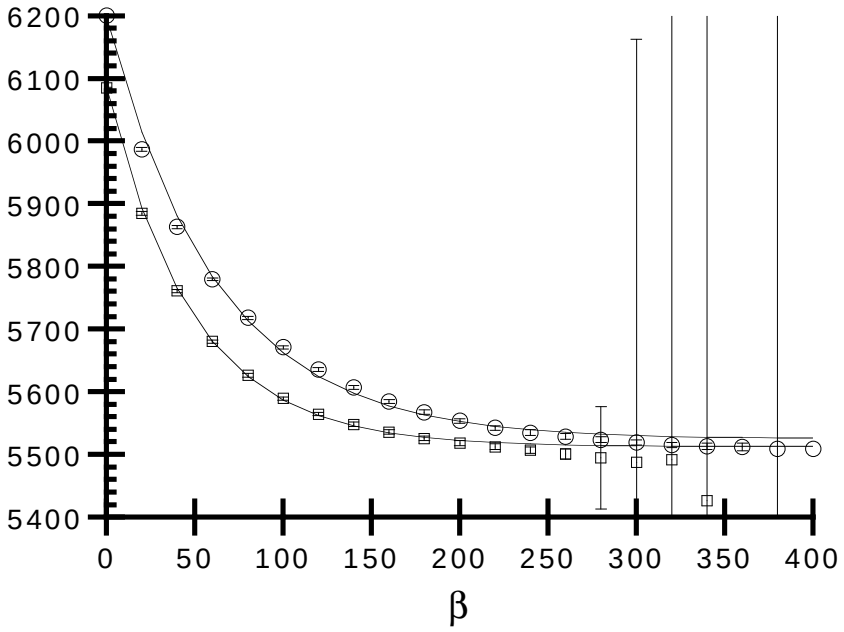

FIG. 4. Convergence of the lowest energy state to the ground state energy as a function of β for the OSS potential. The circles and squares were obtained using 9 and 17 states, respectively. The lines are Marquardt's fits.

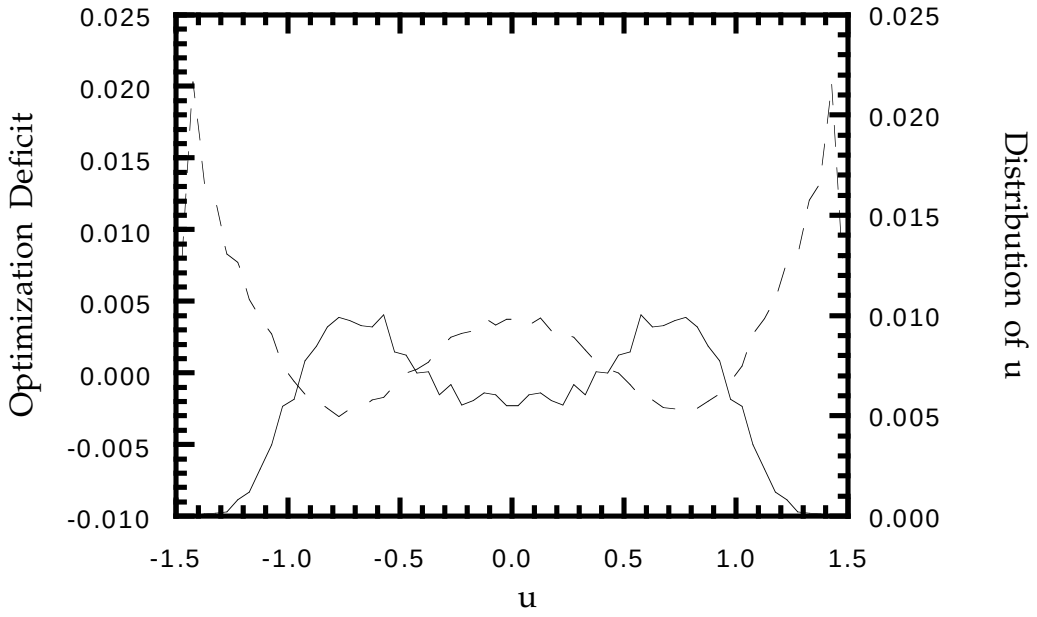

FIG. 5. The OSS VMC distribution of u (solid line) and the f(u) optimization deficit (dashed line) is shown is shown for the two body wavefunction

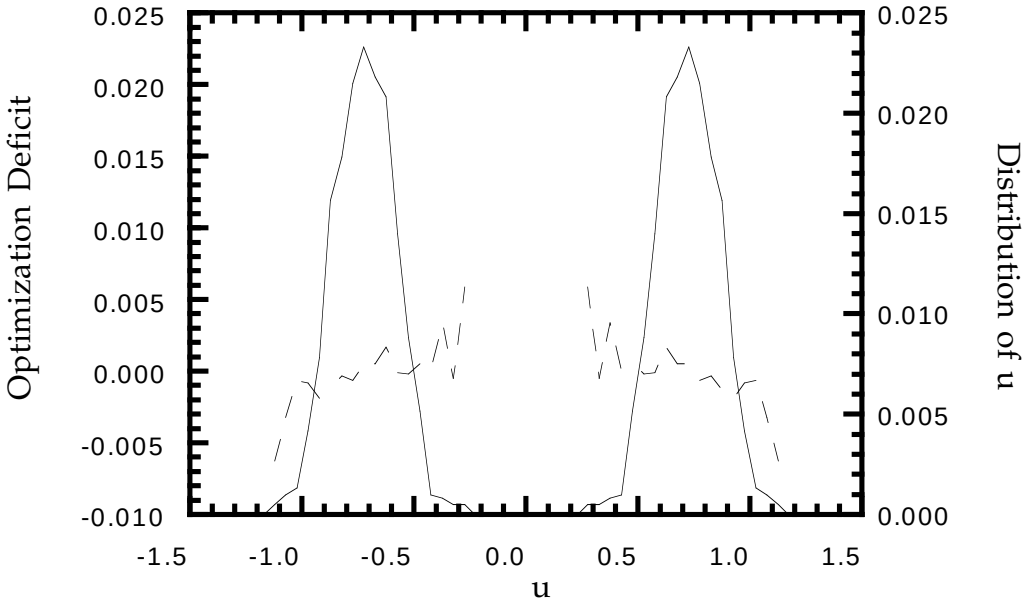

FIG. 6. The OSS VMC distribution of u (solid line) and the f(u) optimization deficit (dashed line) is shown for the two and three body optimized wavefunction

TABLES

TABLE I. Comparison of SSH and OSS potentials with B3LYP hybrid density functional theory calculations of Martin, Hay, and Pratt.[a]

Quantity	SSH	OSS	*ab initio*[a]
H+ Binding on H2O	0.269 Hartree	0.1695 Hartree	0.27367 Hartree
H3O+ Inversion Barrier	4.78 kcal/mole	4.42 kcal/mole	2 kcal/mole
zero-point (Normal Modes)	0.0339 Hartree	0.0281 Hartree	0.0212 Hartree
zero-point (DMC)	0.03042 Hartree	0.02516 Hartree	

[a] R. L. Martin, P. J. Hay, and L. R. Pratt. J. Phys. Chem. A **102**, 3565 (1998).

TABLE II. Variational Energies for the first 5 states using 9, 17, 46, and 99 functions for the OSS potential. An independent estimate for the zero-point energy of 5522(7)/cm is found using diffusion Monte Carlo. 64 trajectories generating 10,000 configurations were used in the integrals.

States	9	17	46	99
0	6198(2)	6083(4)	5903(4)	5856(4)
1	7638(4)	7213(6)	7001(6)	6905(5)
2	9588(5)	9106(10)	8702(12)	8508(10)
3	10045(6)	9449(12)	8804(8)	8672(7)
4	10176(6)	9677(8)	9269(8)	9105(8)

TABLE III. Variational Energies for the first 5 states using 9, 17, 44, and 94 excited state functions for the SSH potential. An independent estimate for the zero-point energy of 6676(7)/cm is found using diffusion Monte Carlo. 64 trajectories generating 10,000 configurations were used in the integrals.

States	9	17	44	94
0	7241(4)	7112(4)	6974(4)	6939(4)
1	8692(6)	8201(6)	8065(6)	7968(6)
2	10604(6)	10176(10)	9790(8)	9538(8)
3	11498(14)	10746(16)	10043(8)	9885(8)
4	11927(8)	11386(8)	10729(8)	10484(6)

TABLE IV. Density matrix Monte Carlo energies for the first few states using 9 and 17 symmetric excited state functions for OSS. One million configurations where used in density matrix Monte Carlo. The time step was 1 / Hartree. Error bars are 90% confidence intervals. An independent estimate for the zero-point energy of 5522(7)/cm is found using diffusion Monte Carlo.

States	9	17
0	5525(4)	5513(5)
1	6297(10)	6307(5)
2	6883(22)	6881(28)
3	7979(10)	7790(38)
4	8083(18)	8038(20)

TABLE V. Density matrix Monte Carlo energies for the first few states using 9 and 17 symmetric excited state functions for SSH. One million configurations where used in density matrix Monte Carlo. The time step was 1 / Hartree. Error bars are 90% confidence intervals. Some data was not well approximated by a decaying exponential. In this case, the point in the plateau with the smallest standard deviation is given. For this data which is designated by a *, 2 standard deviations are given in parenthesis. An independent estimate for the zero-point energy of 6676(7)/cm is found using diffusion Monte Carlo.

States	9	17
0	6661(5)	6675(4)
1	7437(7)	7406(7)
2	7964(54)*	7934(78)*
3	8912(4)	8918(10)
4	10119(25)	9061(43)*

TABLE VI. Parameters used for the variational ground state wavefunction.

	OSS	SSH
s_{OD}	0.911	0.853
s_{DD}	0.935	0.895
m_{OD}	0.157	0.242
m_{DD}	0.078	0.100
a	9.	10.
b	0.851	0.911